Coherent lensless X-ray imaging

Henry N. Chapman[1] and Keith A. Nugent[2]*

Very high resolution X-ray imaging has been the subject of considerable research over the past few decades. However, the spatial resolution of these methods is limited by the manufacturing quality of the X-ray optics. More recently, lensless X-ray imaging has emerged as a powerful approach that is able to circumvent this limitation. A number of classes of lensless X-ray imaging have been developed so far, with many based on other forms of optics. Here we report the key progress in this area, describe the potential applications for biology and materials science, and discuss the prospect for imaging single molecules using X-ray free-electron lasers.

X-ray crystallography has a record of extraordinary achievement in science, and its impact on the biological sciences has been immense. Crystallography was originally used to numerically construct three-dimensional atomic-resolution images of molecules from the beams diffracted by their crystal forms. However, it was not until the influence of macromolecular crystallography was fully realized that a prominent crystallographer, David Sayre, proposed that the methods of crystallography might be adapted for imaging general non-periodic objects to create a new form of lensless very high spatial resolution imaging[1].

Sayre's idea became the subject of sporadic research over the ensuing period, but a convincing experimental demonstration remained elusive for nearly twenty years. The first reported observation of X-ray diffraction from an isolated object was reported in 1987[2], but it was not until 1999 that an image was recovered from X-ray data[3]. This result stimulated a major international research effort aimed at developing coherent lensless X-ray imaging.

Solving the non-crystallographic phase problem

In 1952, Sayre[4] applied Shannon's recent work on sampling theory to crystal diffraction, and noted that there may be sufficient information to uniquely solve for the diffracting object, if only one could measure diffraction intensities midway between Bragg peaks. It was not until 1980 that Sayre suggested[1] that a single isolated object permits such a higher density sampling scheme, as this non-periodic object produces a continuous X-ray diffraction pattern not restricted only to Bragg peaks. It became plausible, therefore, to apply the formidable successes of crystallography to the study of finite but non-periodic objects, thereby creating a lensless imaging methodology at extraordinary spatial resolution. This is the method now known as coherent diffractive imaging (CDI).

From a more modern perspective, Sayre's early work does not prove that a properly measured far-field diffraction pattern would necessarily yield sufficient information to fully determine an image of the diffracting object, primarily because it does not deal with issues of the independence of the additional measurements. However, independent and more or less contemporaneous theoretical work on the phase problem was being undertaken in the electron- and visible-optics communities. Fienup[5], working independently of Sayre in the area of visible optics, argued that it should be possible to recover an object distribution from its Fourier modulus, and proposed some iterative approaches that built on ideas from electron imaging[6]. Bates[7] argued that apart from some 'trivial' ambiguities in the phase recovery problem (lateral translation of the object, complex conjugation, spatial inversion and absolute phase), the diffraction pattern from an isolated object would almost certainly lead to a unique solution. The residual ambiguity falls within the class of 'homometric' structures, in which different objects have identical diffraction patterns; these rather special objects do indeed exist[8], but the likelihood of them being of practical significance is exceedingly small. Miao and colleagues[9] showed that it is possible to recover images from data in which the total number of intensity measurements exceeds the number of unknown image points, although it is possible that this conclusion may depend on the nature of the other constraints available. In the case of illumination by a field that is coherent but contains a spherical phase curvature (that is, Fresnel diffraction), the methods of Bates have been used to show that the diffracted intensity has a truly unique relationship with the diffracting object[10].

The extension of crystallography to lensless X-ray imaging, as envisaged by Sayre in 1980[1], is implemented by the simple process of measuring the far-field diffraction pattern of an object (Fig. 1a). Numerical techniques are then used to invert this diffraction pattern to recover an image of the object. In doing so, one constructs an imaging system that is devoid of image-forming optical elements, thus promising a spatial resolution that is limited in principle only by the wavelength of the incident light. As Sayre pointed out[1], such a scheme loses a key benefit of crystallography — namely the coherent addition of intensities from the many molecules in the crystal. The dose of X-ray radiation to the object is therefore increased by many orders of magnitude, thus making radiation damage a practical limitation[11].

Data analysis

Figure 1 shows the fundamental CDI geometries, including the original concept for CDI (Fig. 1a), in which an isolated object is illuminated with a highly coherent beam of X-rays and the diffraction pattern produced by the sample is measured in the far-field. Diffraction from an isolated object is very weak in practice, so it is necessary to introduce a beam stop to prevent the direct beam from damaging the detector and to facilitate the dynamic range required to properly measure the diffracted signal.

The algorithmic methods used to recover the image have their origins in electron microscopy through the iterative methods first proposed by Gerchberg and Saxton[6]. In the case of CDI, one iteratively seeks a solution that is consistent with both the measured diffraction pattern and any *a priori* information held about the object, with the most commonly used information being the physical extent of the object, otherwise known as its 'support'[12] (see Box 1). The precise details of the manner in which the algorithm is implemented has been the subject of considerable recent research and, in practice, data is analysed using a variety of methods. For

[1]Centre for Free Electron Laser Science, DESY and University of Hamburg, Hamburg, Germany. [2]ARC Centre of Excellence for Coherent X-ray Science, School of Physics, the University of Melbourne, Victoria 3010, Australia. *e-mail: keithan@unimelb.edu.au
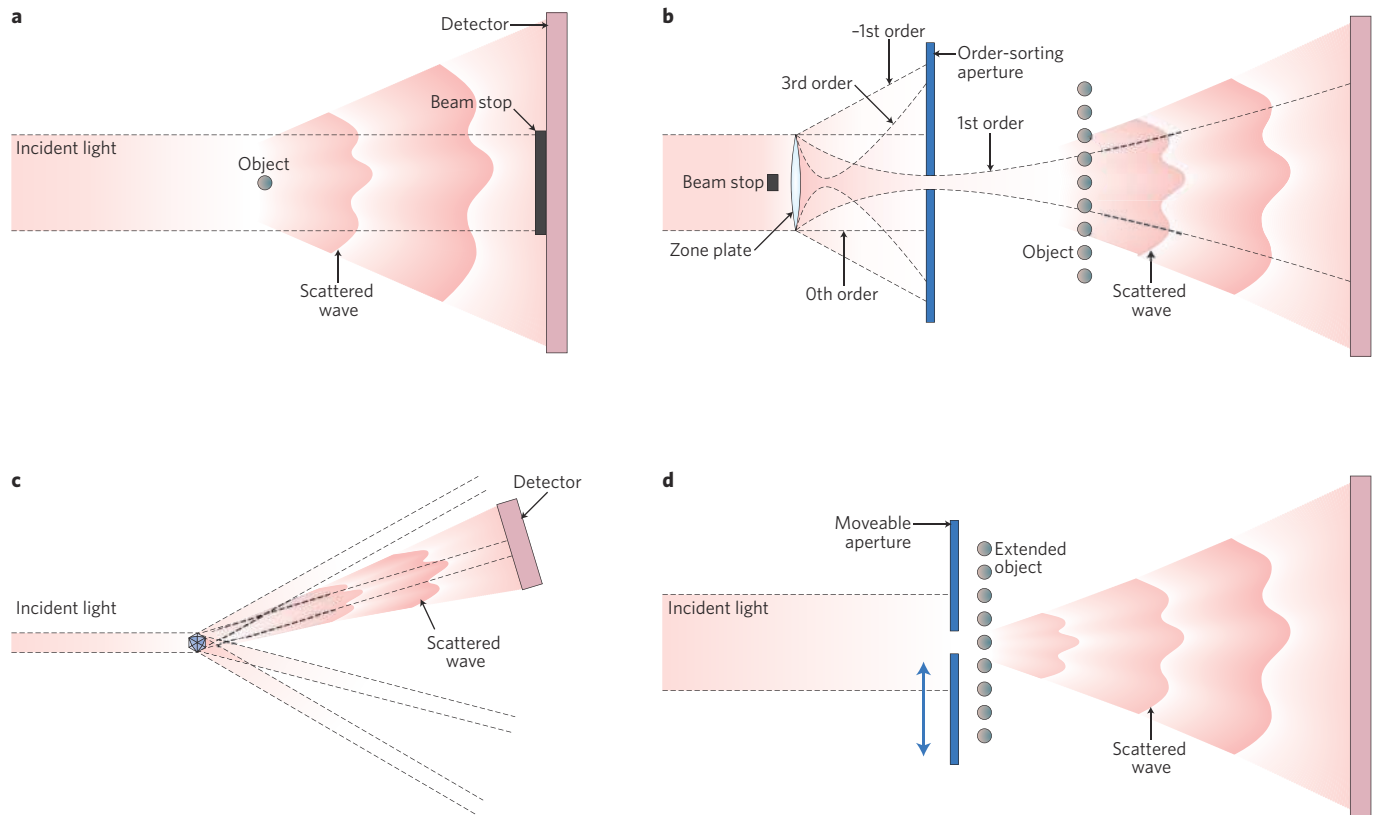
Figure 1 | Experimental configurations for X-ray coherent diffractive imaging. a, Plane-wave CDI, in which a coherent planar beam of X-rays is incident on the sample. **b**, Fresnel CDI, in which a coherent phase-curved beam created by a Fresnel zone plate is incident on the sample. An order-sorting aperture eliminates the unwanted diffracted orders. A beam stop prevents the undiffracted order from passing through the order-sorting aperature. **c**, Bragg CDI, in which a nanocrystal is illuminated and the detailed structure in the Bragg diffraction spots is used to recover information about the shape and strain distribution within the crystal. **d**, Scanning diffraction microscopy, in which a finite beam probe is scanned across the sample and the diffraction pattern observed at each beam position. The finite probe may be formed using a focusing optic such as a Fresnel zone plate.

example, the simple iterative replacement of the latest iterate with *a priori* information (such as the 'known support information') is known as error reduction, the use of a relaxation parameter is known as the hybrid input–output algorithm[13], and there are a range of other important variations on this theme[14]. Perhaps the most interesting innovation in this area is the 'shrink-wrap' algorithm[15], in which the finite support of the object is estimated during the reconstruction process — a method that has found extensive application. These methods have been the subject of recent tutorial reviews by Quiney[16] and Marchesini[17], which also provide interesting and mathematically unified syntheses of the methods.

The algorithms assume a Fourier transform relationship between the field leaving the object and the field at the detector — an assumption that is only strictly correct in the case that the incident field is perfectly coherent. Williams *et al.*[18] showed that even small deviations from perfect spatial coherence can prevent the data from being reliably analysed, and this may have contributed to the long delay between the original proposal of Sayre and its first experimental demonstration with X-rays, with the required coherence only becoming available with modern synchrotron facilities. However, Whitehead *et al.*[19] have successfully modified the algorithms discussed here to account for the effects of partial spatial coherence, thus providing potentially greater throughput and more reliable imaging.

A number of other geometries have either emerged or been subject to a renaissance over the past decade, and one may now discern a number of distinct classes of coherent X-ray imaging methods. The first of these, referred to here as forward-scattering

CDI, conforms to the initial vision of Sayre as it involves the sample being illuminated by a coherent beam and its diffraction pattern being observed along the axis of the incident beam, which can be planar (Fig. 1a) or curved (Fig. 1b). A second class — here termed Bragg CDI — involves illuminating a small crystal and analysing the structure of the Bragg spots to elicit information concerning the shape and internal structure of the crystal, including its strain properties (Fig. 1c). The third class we refer to here as 'scanning CDI'. This is the result of a resurgence of interest in the ptychographic method of electron microscopy[20], in which the image is reconstructed from a set of diffraction patterns obtained while the finite illumination is scanned across an extended sample (Fig. 1d).

X-ray Fourier transform holography has also been subject to renewed attention and can rightly now also be considered under the rubric of coherent lensless imaging methods. However, the development and applications of X-ray holography require considerably more discussion than can be covered here, so this topic is only briefly covered.

Here we discuss each of these approaches before considering the role they might play in an X-ray free-electron laser source.

Forward-scattering CDI

The elementary geometry for forward-scattering CDI is shown in Fig. 1a. The condition for a unique solution is that the beam immediately exiting the object must be finite in spatial extent, thus requiring the sample to be completely isolated in the case of a planar incident beam. In practice, an intense and undiffracted beam
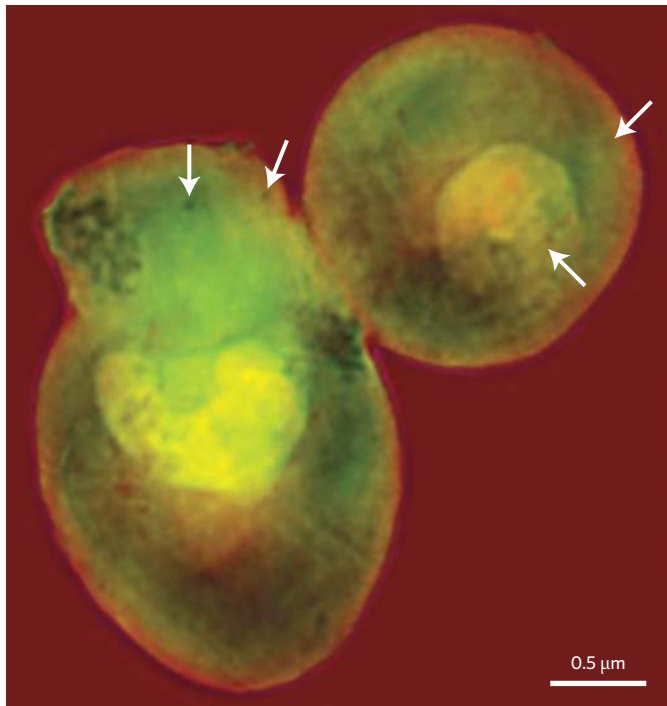
Figure 2 | Biological imaging is an important area for applications of CDI. Optical soft-X-ray image of a yeast cell. The reconstructed complex wave is represented using brightness for magnitude and hue for phase. The arrows indicate the location of immunogold labels. Figure reproduced with permission from ref. 30, © 2010 PNAS.


Figure 3 | Bragg CDI is able to recover the three-dimensional shape and strain structure from a nanocrystal. The shape of a gold nanocrystal and the distribution of the phase shift produced by the strain field from within the nanocrystal are shown. Figure reproduced with permission from ref. 45, © 2006 NPG.

requires the use of a beam stop (or strong attenuator, which has not yet been realized) to prevent it from damaging the detector. The beam stop therefore prevents the measurement of the intensity of the small diffracted angles that scatter within its solid angle. However, as in crystallography, the fundamental experimental configuration is extremely simple.

Nugent *et al.*[21] noted that the capability of modern X-ray optics to produce such small focused beams conceivably allows them to introduce significant phase curvature even for molecule-sized objects. Such beams would create a Fresnel diffraction pattern at the detector plane, a pattern that uniquely defines the phase to within a constant and physically meaningless offset[10] (Fig. 1b). Williams *et al.*[22] experimentally demonstrated the use of Fresnel CDI. The advantage of the Fresnel approach lies in the reliability and consistency of the convergence of the iterative technique[23]. However, producing the incident curved wave introduces some experimental complexity.

Miao and colleagues demonstrated the first reconstruction of three-dimensional images[24], and Chapman *et al.*[25] extended this method to use a full range of projections, resulting in a full tomographic reconstruction. In the work of Chapman *et al.*, the iterative approach was applied directly to the three-dimensional set of diffraction data. The use of a focused beam has also been used to increase the illumination of the sample, and very high spatial resolutions have been reported for simple objects using refractive lenses[26] and X-ray mirror systems[27]. An important additional innovation was demonstrated by Abbey *et al.*[28], in which it was shown that a finite expanding beam can be used to define a finite extent for the wavefield leaving the object, with the result that, in this configuration, CDI is not limited to objects of finite extent, thereby removing an important limitation of coherent imaging methods.
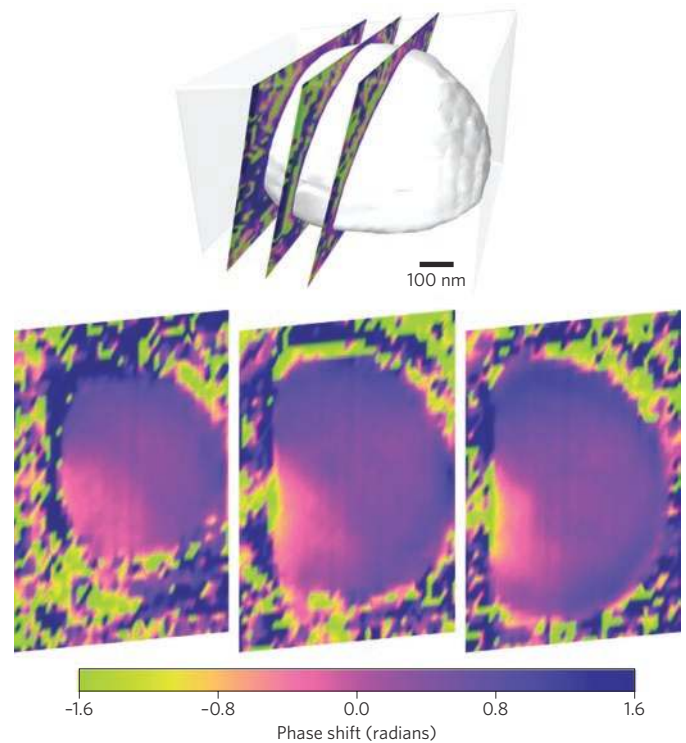
Another motivation for developing the forward-scattering method is its potential for the high-resolution imaging of biological samples, with the first example being from Miao *et al.*[29], among others[30,31] (Fig. 2). Researchers at the Advanced Light Source in California, USA, have compared their image of a yeast cell with an image from a scanning transmission X-ray microscope (see ref. 32, in this issue)[33]. Subsequent work has demonstrated the imaging of frozen hydrated samples, which suggests that real biological applications might be around the corner[34,35]. The use of a curved incident beam has also led to the suggestion that it might be possible to amalgamate scanning X-ray fluorescence microscopy (and other imaging modalities) with high-resolution CDI[36]. Forward-scattering CDI has also been used to produce an image of a chromosome using 8 keV X-rays[37], along with a range of other biological targets.

As with other forms of X-ray microscopy, the significant problem of radiation damage[11] is likely to limit the achievable resolution, particularly for biological materials. These considerations are eased somewhat when non-biological samples are imaged. Barty and colleagues[38] obtained a three-dimensional high-resolution image of a ceramic nanofoam and showed that the image was consistent with the reduced statistical information of its structure obtained from incoherent small-angle X-ray scattering methods, and Abbey *et al.*[39] obtained images of buried structures in an integrated circuit.

Other forms of X-ray sources are also emerging, with laser-driven high-harmonic sources[40] showing consistent improvement. A major goal for these is to achieve substantial emission in the 'water window' region of X-rays, where biological samples show natural contrast due to the different absorption properties of carbon and oxygen (see ref. 32, in this issue). Forward-scattering CDI

835
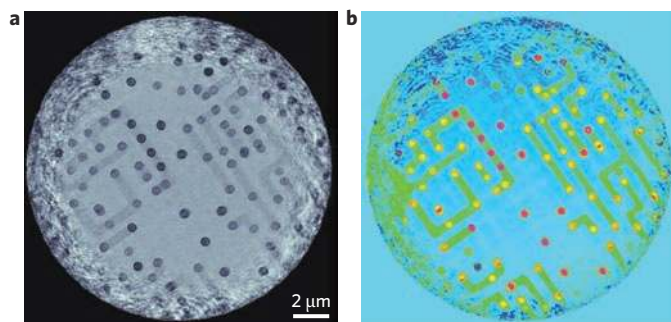
Figure 4 | Scanning diffraction microscopy is able to recover images of extended objects. a,b, Amplitude (**a**) and phase (**b**) distribution of an integrated circuit sample used as a test object. The form of the illuminating probe can also be recovered during the iterative image reconstruction scheme. The pixel size is 36 nm and the sample is 200 μm thick. The X-ray energy used was 7.11 keV. Images courtesy of Pierre Thibault from the Technical University of Munich, Germany.

Figure 5 | Holographic reconstructions of a sample containing bit-patterned magnetic media. a,b, The bits consist of a substrate with 80 nm × 80 nm elevated squares in a 120 nm pitch array, coated with a magnetic multilayer film [Co(5.5 Å)/Pd(9 Å)]$_{24}$ plus seed and cap layers. The black/white contrast is based on X-ray circular dichroism and corresponds to the local magnetization in the magnetic film pointing up/down. Two magnetic states at different points within a magnetization cycle are shown. Images courtesy of Stefan Eisebitt from the Technical University of Berlin, Germany.

has been demonstrated for these sources[41], as well as extensions that permit a number of harmonics to be utilized simultaneously and so increase the useable radiation flux[42].
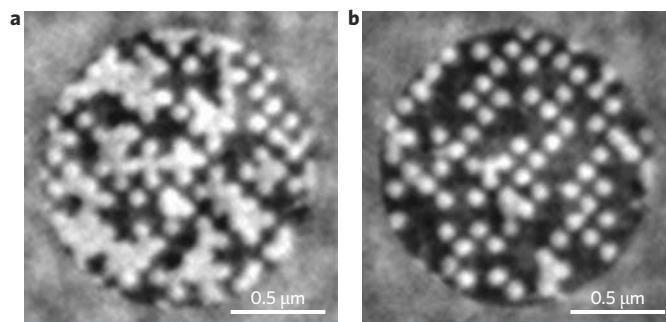
Bragg CDI

CDI originates from the desire to extend the ideas of crystallography to non-periodic samples. However, one of the most productive applications of CDI has been in the study of nanocrystals.

The diffraction pattern of an infinite crystal is the product of the reciprocal lattice with the molecular transform. Elementary Fourier analysis tells us that the diffracted field from a finite crystal differs in that the infinite reciprocal lattice is now convolved with the Fourier transform of the crystal shape — the resulting diffraction pattern is therefore the familiar crystalline diffraction pattern but with a distribution of intensity at the location of what would otherwise be a Bragg diffraction spot. Robinson and colleagues[43] recognized the importance of this information in the study of nanocrystals and showed that it is possible to deduce the detailed shape of a nanocrystal from the shape of the Bragg spots produced by the crystal.

A slight tilting of the crystal will have the effect of rapidly moving the diffraction spot through the diffraction condition[44], making it simple to obtain a three-dimensional measurement of the Bragg spot distribution and therefore obtain information about the three-dimensional shape of the nanocrystal. Again, elementary Fourier analysis tells us that the imposition of simple shape information on a periodic sample will result in a centrosymmetric Bragg spot distribution. However it was observed that the spots rarely display the expected symmetry, which implies that the shape function must be complex. The phase information arises from strains within the crystal, thus allowing Bragg CDI to yield very high resolution three-dimensional images of strain from within a nanocrystal (Fig. 3), in the direction of the reciprocal lattice vector[45]. The Bragg diffraction used to form the pattern has the interesting trait that the object does not need to be physically isolated, as a non-periodic substrate (for example) will be invisible to the diffraction process. As a result, one can use this method to study the impact of an interface with the crystal under study. A long-term goal of Bragg CDI is to image the strain tensor by combining information from several Bragg spots, and perhaps to coherently combine many Bragg spots to obtain atomic-resolution images of the whole crystal. A useful overview of this field has been published by Robinson and Harder[46].

Scanning diffraction microscopy (ptychography)

The phase problem for imaging has been known for many years

and was seriously addressed by the electron imaging community. Ptychography is a method that was proposed in the 1960s for solving the phase problem in transmission electron microscopy[47]. The fundamental idea is to pass a probe beam (a focused or apertured beam, for example) over a sample and to record the resulting two-dimensional diffraction pattern as a function of the beam position. In the typical case of a two-dimensional scan of the beam, the result is a four-dimensional set of data. The dataset is separable into the four-dimensional Wigner functions of the probe and the sample[47], and knowledge of the probe allows the direct retrieval of the phased diffraction wavefield of the sample, as was experimentally demonstrated in ref. 48. Iterative methods based on the ideas outlined in this Review have been developed; these have eased the computational burden[49] and have now been experimentally demonstrated[50]. This approach joins the work of Abbey *et al.*[28] in opening up lensless X-ray imaging to extended samples (Fig. 4). A further extension has been suggested in which an intermediate iterative step is included that permits the probe beam distribution to be obtained[51], therefore allowing a further improvement in the achievable resolution.

The large amount of redundant data obtained in ptychography allows it to produce reliable and quantitative images of extended objects. This also allows ptychography to account for partial coherence[47], making it promising for lensless imaging using synchrotron sources. Some interesting and potentially valuable biological imaging results are now beginning to emerge[52].

Fourier transform holography

X-ray holography — the first coherent imaging technique identified for use with X-rays — has a history that is too extensive to be covered adequately by this Review. In holographic imaging, the wave scattered by an object interferes with a known reference wave and thus allows direct and deterministic recovery of the image information. This is in contrast with the methods that are the main subject of this Review, in which no reference wave is needed and the images are recovered using an iterative phase-recovery method. Nonetheless, it can be argued that this topic should be covered, if only briefly, in a discussion of coherent lensless imaging.

X-ray Fourier transform holographic methods were first demonstrated[53] in the 1980s, and the advent of high-coherence X-ray sources has enabled these methods to find some important areas of application — the most important of which is the study of

Box 1 | Iterative phase retrieval

The far-field diffraction pattern of an object with a transmission $f(x)$ can be represented by its Fourier transform

$$F(u) = \mathbf{F}\{f(x)\} = \int f(x) \exp(-2\pi i x u) \, dx$$

such that the inverse Fourier transform synthesizes the image of $f(x)$ from its complex Fourier components $F(u)$:

$$f(x) = \mathbf{F}^{-1}\{F(u)\} = \int F(u) \exp(2\pi i x u) \, du$$

However, the phase $\varphi(u)$ of the wavefield cannot be directly measured in the X-ray regime and must be recovered before the synthesis can be performed. This inverse problem is equivalent to determining $f(x)$ from samples of $|F(u)|$ by applying available *a priori* knowledge about $f(x)$. One of the strongest constraints that can be applied is that the object has a finite support, outside of which $f(x)$ should vanish; that is, the sum of all the frequencies $|F(u)|\exp(i\varphi(u))\exp(2\pi i x u)$ is zero outside this region (represented by the set S). The application of this constraint requires the diffraction pattern $|F(u)|$ to be measured finely enough to properly sample diffraction fringes that would occur from (the non-existent) scattering points in this region.

The simplest iterative scheme — Fienup's error reduction — starts from a random guess of $\varphi(u)$ to give $F_1' = |F(u)|\exp(i\varphi_1(u))$. The image $f_1'(x)$ is then formed by inverse transformation. This will not be zero outside the support, so the estimate of the image is updated by setting $f_2(x)$ equal to $f_1'(x)$ in the support, and zero elsewhere. This is then transformed to a new diffraction pattern $F_2(u)$. However, $F_2(u)$ will not conform to the measured amplitudes, and is therefore set to $F_2'(u) = |F(u)|\exp(i\varphi_2(u))$, which is transformed

back to form $f_2'(x)$. This is repeated by alternately applying the 'Fourier modulus constraint':

$$f_n'(x) = \mathbf{F}^{-1}\{|F(u)|\exp(i \arg(\mathbf{F}[f_n(x)]))\}$$

and the 'support constraint':

$$f_{n+1}(x) = f_n'(x) \ \text{if} \ x \in S$$
$$f_{n+1}(x) = 0 \ \text{if} \ x \notin S$$

This algorithm can be more compactly written in terms of projection operators, $f_{n+1}(x) = P_S P_M f_n(x)$, where P_M performs the first part of the iteration (the Fourier modulus constraint) and P_S performs the second (the support constraint). The solution occurs when both constraints are satisfied — that is, $P_S f_n(x) = P_M f_n(x)$ — but Fienup's error reduction often stagnates without reaching this solution. This is because the application of projection operators always minimizes the error between the iterate and constraint, thus leaving no recourse to escape the local minima of the solution space. A common problem is the stagnation at the sum of the correct image and its centrosymmetrical inversion (either of which is a valid solution, but not both). Zeroes in the diffraction intensities are problematic because the projection P_M is not well-defined at those points. Often the incorrect locations of pairs of phase vortices (branch cuts of the complex-valued field) in the diffraction pattern cause stripes in the reconstructed image, which form a deep local minimum. Modifications of the iterative schemes aim to avoid these stagnations, and Elser's difference map[14] formally avoids this case. Other constraints, such as positivity or atomicity, can be applied in a similar way.

magnetic samples, beginning with the work of Eisebitt *et al.*[54] Figure 5 shows examples of results obtained using this method.

It is important to note that the work of the coherent diffraction community has led to considerable development of Fourier transform holography. Of particular importance is the use of multiple reference sources[55] and complex structured sources such as the uniformly redundant array[56], a structure comprising a distribution of pinholes that produces a perfectly flat power spectrum. It is hoped that these approaches will enable improved spatial resolution by creating a small characteristic scale in the reference source while retaining a large open area.

A particularly interesting hybrid approach that draws extensively from the ideas of CDI has arisen from the work of Podorov *et al.*[57], in which diffraction is from the edge of an aperture instead of from the pinhole reference source used in Fourier transform holography. In this way, the resolution of the reconstructed image is limited by, for example, the straightness with which an edge may be constructed, thus potentially allowing very high spatial resolution holographic imaging. This method has been generalized by the work of Guizar-Sicairos and Fienup[58], and has been experimentally demonstrated for the imaging of magnetic samples[59].

X-ray free-electron lasers

Imaging molecular-scale structures using X-ray free-electron lasers[60] was proposed as a possible solution to the problem of radiation damage, which limits the achievable resolution of lensless X-ray imaging. This imaging method involves subjecting a stream of single molecules to X-ray laser pulses and observing the diffracted X-rays. Although the pulses are intense enough to cause molecular disintegration, they are sufficiently short such that the diffraction process will be complete before the molecules have undergone significant structural change.

Although this method is simple in concept, substantial problems still remain. The open questions are associated with the ability to acquire adequate data, whether the molecule will disintegrate before the diffraction process is completed, and the problem of assembling all of the data from the different random molecular orientations into a consistent single set of data.

Progress so far has been encouraging. The fundamental problem of recovering the electron distribution from a continuous diffraction pattern has been thoroughly demonstrated, as is evidenced by the literature cited in this Review. Furthermore, the standard methods of crystallography, such as multiwavelength anomalous dispersion and heavy atom replacement, remain as potential tools for use with X-ray free-electron lasers. Chapman *et al.*[61], using the FLASH free-electron laser in Hamburg, Germany, have experimentally demonstrated that it is possible to recover the structure of a sample before it disintegrates. CDI has been used to produce images of the disintegration of a sample after illumination from a free-electron laser[62], and these studies have yielded results that are consistent with the motion predicted by dynamics codes. The nuclear motion of a disintegrating biomolecule has been studied computationally, and it now seems safe to anticipate that motion is negligible on timescales shorter than around 5 fs (refs 63,64). However, electron damage might happen on an even shorter timescale than this, and the impact of such damage is the subject of ongoing study.

The classification of the very low signal diffraction patterns into their orientations is another challenging problem, and the methods of single-particle electron diffraction are unlikely to be suitable. However, a recent proposal by Fung *et al.*[65] suggests that the use of sophisticated Bayesian statistics offers a path forward, and it might also be possible to align the molecules through laser methods[66], for example.

837

The problems that currently stand in the way of imaging biomolecules using free-electron laser pulses are being steadily solved by the international research community, and there is every reason at the moment to anticipate the success of this endeavour.

Summary

The field of X-ray lensless imaging has seen significant growth over the past decade. CDI imaging can be applied to many important problems and we now know how the method may be applied to extended objects with very high spatial resolution, the determination of strain distributions in crystalline samples, and the visualization of magnetic structures using holographic methods. These possibilities have arisen through the wealth of recent new ideas. We believe it is safe to assert that CDI and its related methods can now be regarded as an established form of high-resolution imaging using coherent X-ray sources.

The goal of imaging single, clusters or nanocrystals of biomolecules is still just out of reach. The obstacles are now yielding, however, thanks to intensive research and to a barrage of new ideas. We believe that there is an excellent chance that this goal can be achieved in the foreseeable future. It promises rewards in structural biology, condensed matter physics, magnetism and other correlated systems, as well as for the detailed investigation of matter under extreme conditions.

References

1. Sayre, D. in *Imaging Processes and Coherence in Physics* Vol. 112 (eds Schlenker, A. *et al.*) 229–235 (Springer, 1980).
2. Yun, W. B., Kirz, J. & Sayre, D. Observation of the soft X-ray diffraction pattern of a single diatom. *Acta Crystallogr. A* **43,** 131–133 (1987).
3. Miao, J. W., Charalambous, P., Kirz, J. & Sayre, D. Extending the methodology of X-ray crystallography to allow imaging of micrometre-sized non-crystalline specimens. *Nature* **400,** 342–344 (1999).
4. Sayre, D. Some implications of a theorem due to Shannon. *Acta Crystallogr.* **5,** 843–843 (1952).
5. Fienup, J. R. Reconstruction of an object from modulus of its Fourier-transform. *Opt. Lett.* **3,** 27–29 (1978).
6. Gerchberg, R. W. & Saxton, W. O. Practical algorithm for determination of phase from image and diffraction plane pictures. *Optik* **35,** 237–246 (1972).
7. Bates, R. H. T. Fourier phase problems are uniquely solvable in more than one dimension: Underlying theory. *Optik* **61,** 247–262 (1982).
8. Nugent, K. A., Peele, A. G., Quiney, H. M. & Chapman, H. N. Diffraction with wavefront curvature: A path to unique phase recovery. *Acta Crystallogr. A* **61,** 373–381 (2005).
9. Miao, J., Sayre, D. & Chapman, H. N. Phase retrieval from the magnitude of the Fourier transforms of nonperiodic objects. *J. Opt. Soc. Am. A* **15,** 1662–1669 (1998).
10. Pitts, T. A. & Greenleaf, J. F. Fresnel transform phase retrieval from magnitude. *IEEE T. Ultrason. Ferr.* **50,** 1035–1045 (2003).
11. Howells, M. R. *et al.* An assessment of the resolution limitation due to radiation-damage in X-ray diffraction microscopy. *J. Electron Spectrosc.* **170,** 4–12 (2009).
12. Fienup, J. R. Reconstruction of a complex-valued object from the modulus of its Fourier-transform using a support constraint. *J. Opt. Soc. Am. A* **4,** 118–123 (1987).
13. Fienup, J. R. Phase retrieval algorithms: A comparison. *Appl. Opt.* **21,** 2758–2769 (1982).
14. Elser, V. Phase retrieval by iterated projections. *J. Opt. Soc. Am. A* **20,** 40–55 (2003).
15. Marchesini, S. *et al.* X-ray image reconstruction from a diffraction pattern alone. *Phys. Rev. B* **68,** 140101 (2003).
16. Quiney, H. M. Coherent diffractive imaging using short wavelength light sources: A tutorial review. *J. Mod. Opt.* **57,** 1109–1149 (2010).
17. Marchesini, S. A unified evaluation of iterative projection algorithms for phase retrieval. *Rev. Sci. Instrum.* **78,** 011301 (2007).
18. Williams, G. J., Quiney, H. M., Peele, A. G. & Nugent, K. A. Coherent diffractive imaging and partial coherence. *Phys. Rev. B* **75,** 104102 (2007).
19. Whitehead, L. W. *et al.* Diffractive imaging using partially coherent X-rays. *Phys. Rev. Lett.* **103,** 243902 (2009).
20. Hoppe, W. Diffraction in inhomogeneous primary wave fields: Principle of phase determination from electron diffraction interference. *Acta Crystallogr. A* **25,** 495–501 (1969).
21. Nugent, K. A., Peele, A. G., Chapman, H. N. & Mancuso, A. P. Unique phase recovery for nonperiodic objects. *Phys. Rev. Lett.* **91,** 203902 (2003).
22. Williams, G. J. *et al.* Fresnel coherent diffractive imaging. *Phys. Rev. Lett.* **97,** 025506 (2006).
23. Quiney, H. M., Nugent, K. A. & Peele, A. G. Iterative image reconstruction algorithms using wave-front intensity and phase variation. *Opt. Lett.* **30,** 1638–1640 (2005).
24. Miao, J. W. *et al.* High resolution 3D X-ray diffraction microscopy. *Phys. Rev. Lett.* **89,** 088303 (2002).
25. Chapman, H. N. *et al.* High-resolution *ab initio* three-dimensional X-ray diffraction microscopy. *J. Opt. Soc. Am. A* **23,** 1179–1200 (2006).
26. Schroer, C. G. *et al.* Coherent X-ray diffraction imaging with nanofocused illumination. *Phys. Rev. Lett.* **101,** 090801 (2008).
27. Takahashi, Y. *et al.* High-resolution diffraction microscopy using the plane-wave field of a nearly diffraction limited focused X-ray beam. *Phys. Rev. B* **80,** 054103 (2009).
28. Abbey, B. *et al.* Keyhole coherent diffractive imaging. *Nature Phys.* **4,** 394–398 (2008).
29. Miao, J. W. *et al.* Imaging whole *Escherichia coli* bacteria by using single-particle X-ray diffraction. *Proc. Natl Acad. Sci. USA* **100,** 110–112 (2003).
30. Nelson, J. *et al.* High-resolution X-ray diffraction microscopy of specifically labeled yeast cells. *Proc. Natl Acad. Sci. USA* **107,** 7235–7239 (2010).
31. Jiang, H. D. *et al.* Quantitative 3D imaging of whole, unstained cells by using X-ray diffraction microscopy. *Proc. Natl Acad. Sci. USA* **107,** 11234–11239 (2010).
32. Sakdinawat, A. & Attwood, D. Nanoscale X-ray imaging. *Nature Photon.* **4,** 840–848 (2010).
33. Shapiro, D. *et al.* Biological imaging by soft X-ray diffraction microscopy. *Proc. Natl Acad. Sci. USA* **102,** 15343–15346 (2005).
34. Huang, X. J. *et al.* Soft X-ray diffraction microscopy of a frozen hydrated yeast cell. *Phys. Rev. Lett.* **103,** 198101 (2009).
35. Lima, E. *et al.* Cryogenic X-ray diffraction microscopy for biological samples. *Phys. Rev. Lett.* **103,** 198102 (2009).
36. Williams, G. J. *et al.* High-resolution X-ray imaging of *Plasmodium falciparum*-infected red blood cells. *Cytom. Part A* **73A,** 949–957 (2008).
37. Nishino, Y., Takahashi, Y., Imamoto, N., Ishikawa, T. & Maeshima, K. Three-dimensional visualization of a human chromosome using coherent X-ray diffraction. *Phys. Rev. Lett.* **102,** 018101 (2009).
38. Barty, A. *et al.* Three-dimensional coherent X-ray diffraction imaging of a ceramic nanofoam: Determination of structural deformation mechanisms. *Phys. Rev. Lett.* **101,** 055501 (2008).
39. Abbey, B. *et al.* Quantitative coherent diffractive imaging of an integrated circuit at a spatial resolution of 20 nm. *Appl. Phys. Lett.* **93,** 214101 (2008).
40. Ditmire, T. *et al.* Spatial coherence measurement of soft X-ray radiation produced by high order harmonic generation. *Phys. Rev. Lett.* **77,** 4756–4759 (1996).
41. Sandberg, R. L. *et al.* Lensless diffractive imaging using tabletop coherent high-harmonic soft-X-ray beams. *Phys. Rev. Lett.* **99,** 098103 (2007).
42. Chen, B. *et al.* Multiple wavelength diffractive imaging. *Phys. Rev. A* **79,** 023809 (2009).
43. Robinson, I. K., Vartanyants, I. A., Williams, G. J., Pfeifer, M. A. & Pitney, J. A. Reconstruction of the shapes of gold nanocrystals using coherent X-ray diffraction. *Phys. Rev. Lett.* **8719,** 195505 (2001).
44. Williams, G. J., Pfeifer, M. A., Vartanyants, I. A. & Robinson, I. K. Three-dimensional imaging of microstructure in Au nanocrystals. *Phys. Rev. Lett.* **90,** 175501 (2003).
45. Pfeifer, M. A., Williams, G. J., Vartanyants, I. A., Harder, R. & Robinson, I. K. Three-dimensional mapping of a deformation field inside a nanocrystal. *Nature* **442,** 63–66 (2006).
46. Robinson, I. & Harder, R. Coherent X-ray diffraction imaging of strain at the nanoscale. *Nature Mater.* **8,** 291–298 (2009).
47. Rodenburg, J. M. & Bates, R. H. T. The theory of superresolution electron-microscopy via Wigner-distribution deconvolution. *Phil. Trans. R. Soc. Lond. A* **339,** 521–553 (1992).
48. Chapman, H. N. Phase-retrieval X-ray microscopy by Wigner-distribution deconvolution. *Ultramicroscopy* **66,** 153–172 (1996).
49. Faulkner, H. M. L. & Rodenburg, J. M. Movable aperture lensless transmission microscopy: A novel phase retrieval algorithm. *Phys. Rev. Lett.* **93,** 023903 (2004).
50. Rodenburg, J. M. *et al.* Hard-X-ray lensless imaging of extended objects. *Phys. Rev. Lett.* **98,** 034801 (2007).
51. Thibault, P. *et al.* High-resolution scanning X-ray diffraction microscopy. *Science* **321,** 379–382 (2008).

52. Giewekemeyer, K. *et al.* Quantitative biological imaging by ptychographic X-ray diffraction microscopy. *Proc. Natl Acad. Sci. USA* **107,** 529–534 (2010).
53. McNulty, I. *et al.* High-resolution imaging by Fourier-transform X-ray holography. *Science* **256,** 1009–1012 (1992).
54. Eisebitt, S. *et al.* Lensless imaging of magnetic nanostructures by X-ray spectro-holography. *Nature* **432,** 885–888 (2004).
55. Schlotter, W. F. *et al.* Multiple reference Fourier transform holography with soft X-rays. *Appl. Phys. Lett.* **89,** 163112 (2006).
56. Marchesini, S. *et al.* Massively parallel X-ray holography. *Nature Photon.* **2,** 560–563 (2008).
57. Podorov, S. G., Pavlov, K. M. & Paganin, D. M. A non-iterative reconstruction method for direct and unambiguous coherent diffractive imaging. *Opt. Express* **15,** 9954–9962 (2007).
58. Guizar-Sicairos, M. & Fienup, J. R. Holography with extended reference by autocorrelation linear differential operation. *Opt. Express* **15,** 17592–17612 (2007).
59. Zhu, D. L. *et al.* High-resolution X-ray lensless imaging by differential holographic encoding. *Phys. Rev. Lett.* **105,** 043901 (2010).
60. Neutze, R., Wouts, R., van der Spoel, D., Weckert, E. & Hajdu, J. Potential for biomolecular imaging with femtosecond X-ray pulses. *Nature* **406,** 752–757 (2000).
61. Chapman, H. N. *et al.* Femtosecond diffractive imaging with a soft-X-ray free-electron laser. *Nature Phys.* **2,** 839–843 (2006).
62. Hau-Riege, S. P. *et al.* Sacrificial tamper slows down sample explosion in FLASH diffraction experiments. *Phys. Rev. Lett.* **104,** 064801 (2010).
63. Hau-Riege, S. P., London, R. A., Huldt, G. & Chapman, H. N. Pulse requirements for X-ray diffraction imaging of single biological molecules. *Phys. Rev. E* **71,** 061919 (2005).
64. Jurek, Z., Oszlanyi, G. & Faigel, G. Imaging atom clusters by hard X-ray free-electron lasers. *Europhys. Lett.* **65,** 491–497 (2004).
65. Fung, R., Shneerson, V., Saldin, D. K. & Ourmazd, A. Structure from fleeting illumination of faint spinning objects in flight. *Nature Phys.* **5,** 64–67 (2009).
66. Spence, J. C. H. & Doak, R. B. Single molecule diffraction. *Phys. Rev. Lett.* **92** (2004).

Acknowledgements

Additional information

The authors declare no competing financial interests.